Quantification of Solvent Water and Hydration Dynamic of Thermo-Sensitive Microgel by Dielectric Spectroscopy

Man Yang, Wenjuan Su, Kongshuang Zhao

College of Chemistry, Beijing Normal University, Beijing 100875, China
Correspondence to: K. Zhao (E-mail: zhaoks@bnu.edu.cn)

Received 6 May 2017; revised 16 August 2017; accepted 6 September 2017; published online 11 October 2017
DOI: 10.1002/polb.24513

ABSTRACT: The hydration of natural or synthetic macromolecules is of fundamental importance in our understanding of their structure and stability. Quantification of hydration water can promote the understanding to many complex biological mechanisms such as protein folding, as well as the dynamics and conformation of polymers. An approach to quantification of solvent water was developed by dielectric spectroscopy. Dielectric behaviors of PNIPAM microgels with different crosslink density distribution were measured in the range of 0.5–40 GHz and 15–50. An obvious relaxation process caused by free and bound water was found. Dielectric parameters of free and bound water show that the crosslink density distribution does not affect the volume phase transition temperature of microgels, but significantly influence the orientation dynamics of the solvent water. We found that the three kinds of microgel can be distinguished by the dielectric parameters of the bound water. In addition, the number of water in and outside microgel during the volume phase transition process was quantitatively calculated for the first time. This study provides the possibility for the quantification of water in complex biological process. © 2017 Wiley Periodicals, Inc. J. Polym. Sci., Part B: Polym. Phys. **2017**, *55*, 1859–1864

KEYWORDS: bound water; dielectric properties; dielectric relaxation; hydration dynamics; microgels; phase separation; quantification; relaxation; stimuli-sensitive polymers; swelling

INTRODUCTION Water is the most important and active molecule in all biomacromolecules,[1] and it is thought to affect the function, structure, stability, and dynamics of other biological macromolecules.[1–3] Therefore, the quantification of water will undoubtedly promote the understanding of many complex biological mechanisms, such as protein folding.[4] Due to the complex structure of biomacromolecules, some alternatives are often used as model molecules to study some biological processes. Poly(*N*-isopropylacrylamide) (PNIPAM), which is a typical thermosensitive polymer with the lower critical solution temperature (LCST) of 32 °C [for PNIPAM gel, it is called volume phase transition temperature (VPTT)], is often used as a model molecule because of its similar structure with amino acid which is the basic unit of some biomacromolecules such as protein and enzyme.[5,6] In microgel aqueous solution, there are two forms of water, that is, the bound and free water. In some electrolyte and ionic liquid systems,[7–13] the bound water is also classified to rotationally bound water and irrotationally bound water. The main origin of irrotationally bound water is the strong ion–dipole interaction between the ions and solvent, which fix the orientation of the surrounding solvent dipoles.[14] Because the bound water is related to the polymer hydration, the quantification of bound water during the phase transition of microgel, on the one hand, is expected to help us to understand the dynamics and conformation of thermosensitive polymers; on the other hand, it provides an approach to the quantification of hydration water in other biological process, which will undoubtedly speed up the process of exploring the mystery of life phenomena.

In fact, there has been precedent for the quantitative studies of water molecules during the phase transition of PNIPAM. Shikata and coworkers[15–17] determined from dielectric spectroscopy that hydration number of water bound on per monomer below the LCST is 11 and when the temperature is increased to LCST, all the 11 water molecules dehydrated from the monomer unit. This result is close to the value of 13 obtained from differential scanning calorimetry by Shibayama et al.[18,19] Kogure et al.[20] quantitatively evaluated the hydration number bound to one NiPAM monomer in PNIPAM gel by ultrasonic velocity and found that the hydration number at low and high temperatures were about 7.5 (20 °C) and 3 (40 °C), respectively. By quasielastic neutron scattering method, Philipp et al.[21] revealed that the PNIPAM chain is partially dehydrated and the hydration number decreases from 8 to 2 during the phase transition. As can be seen from the above researches, most of these studies concentrate on the dehydration dynamics of the linear PNIPAM

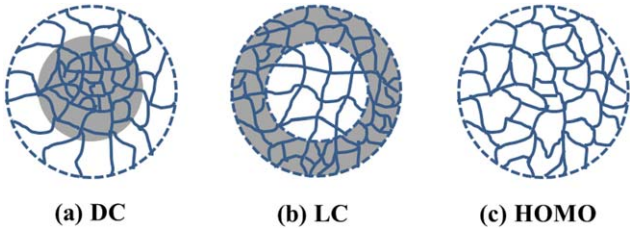

FIGURE 1 Schematic diagram of three types of PNIPAM microgels with different spatial cross-linking density distributions: (a) microgels with a dense core and a loose shell (DC), (b) microgels with a loose core and a dense shell (LC), and (c) microgels with homogenous cross-linking density distribution (HOMO). The darker the color, the higher the cross-linking density. [Color figure can be viewed at wileyonlinelibrary.com]

chain, and rarely involves the microgel. This is because that the PNIPAM chain has clear molecular weight and simple structure, and thus, it is easy to determine the hydration number during the "coil-to-globule" transition. However, due to the complex structure and the difficulty in determining the molecular weight of microgel, it is hard to quantitatively calculate the number of water bound in microgel at the molecular level. What merely known to all is that the water content in the network is up to more than 70%, even in a highly collapsed PNIPAM microgel.[22–24]

To fill the vacancy in the study on the quantification of solvent water in microgel, three kinds of microgels with different crosslink density distribution, dense core and loose shell (DC), loose core and dense shell (LC), and homogenous (HOMO) as shown in Figure 1 were studied by dielectric spectroscopy from 0.5 to 40 GHz as a function of temperature. In particular, we expect to calculate the hydration number of water quantitatively below and above the VPTT and to provide an approach for the quantification of water in other complex biological processes. Besides, our previous study[25] on the same system suggested that the radio frequency dielectric spectroscopy is powerless to distinguish the three kinds of microgel; therefore, another purpose of this work is to distinguish the three microgels from the perspective of solvent water by microwave dielectric spectroscopy.

EXPERIMENTAL

Material

N-Isopropylacrylamide (NIPAM, Fluka) was recrystallized using a 1:1 toluene/*n*-hexane mixture twice. *N*,*N*-Methylenebisacrylamide (MBA, Fluka) was recrystallized by using methanol, and potassium persulfate (KPS, Merck) was used as received. Deionized water was used in all the experiment.

Preparation of PNIPAM Microgels with Different Crosslinking Density Distribution

Three types of nanometer-sized microgels with different spatial distributions of cross-linker were synthesized by combining semibatch and temperature-programmed surfactant-free precipitation polymerization. The structure of the temperature-responsive PNIPAM microgels are shown in Figure 1: microgels with dense-core [DC; Fig. 1(a)], microgels with loose-core [LC; Fig. 1(b)], and homogeneous microgels [HOMO; Fig. 1(c)].[25] The detailed preparation procedure can refer to the literatures.[26] Because the cross-linker content used to synthesize three types of microgels is same, the only difference of these microgel particles is the spatial distributions of cross-linker.

Dielectric Measurements

Dielectric measurements were performed in the frequency range from 0.5 to 40 GHz as a function of temperature by Agilent E8363C PNA series network analyzer (Agilent Technologies). An Agilent 85070E open-ended coaxial probe was used for the dielectric measurements. The microgel solution is measured simply by immersing the probe into the solution. The error of the analyzer is calibrated before measuring the permittivity of the sample by measuring three standards: deionized water, air, and a short circuit. The dielectric constants ε and loss ε'' were automatically calculated as functions of frequency by the built-in software of this measuring system. The temperature is controlled by a thermostat (DC-0506) with a temperature stability of 0.05 K. The concentration of microgel solution used for dielectric measurement is 5 mg/mL.

RESULTS AND DISCUSSION

Dielectric Spectra of Three Kinds of Microgels

All the dielectric spectroscopy of the three kinds of microgels was obtained according to the method described in Dielectric Measurements section. Figure 2 compares the dielectric constant (a) and loss (b) of the microgel systems at room temperature with the pure water (the dielectric spectroscopy at other temperatures is not listed here). An obvious relaxation process was observed at GHz range. Besides, it can be clearly seen from the inset that both the values of dielectric constant and loss of microgel systems are lower than that of pure water (the hollow pentagram), which is a result of the decreased volume fraction of water in the system.

In general, the rotation of pure water will induce a typical Debye relaxation in an external electric field, and the characteristic relaxation time at room temperature is 8.3 ps (19 GHz).[27] Besides, the relaxation of PNIPAM, including the rotational reorientation of side group, usually occurs at frequency below 100 MHz, as indicated by Kita and coworkers and Schönhals.[28,29] Thus, we believe that the relaxation near GHz is caused by the rotational motion of water molecules. It is generally believed that the two different forms of water molecules exist in polymer aqueous solutions, namely, the bound and free water. The former is related to the polymer hydration. In other words, the observed relaxation is actually composed of the contributions from the two forms of water. Because rotationally and irrotationally bound water is usually involved in ionic systems,[7–14] we do not divide bound water into these two kinds of water in the current system. Therefore, the HN eq 1 including two relaxation terms was used to fit the dielectric spectra of the three microgel systems,

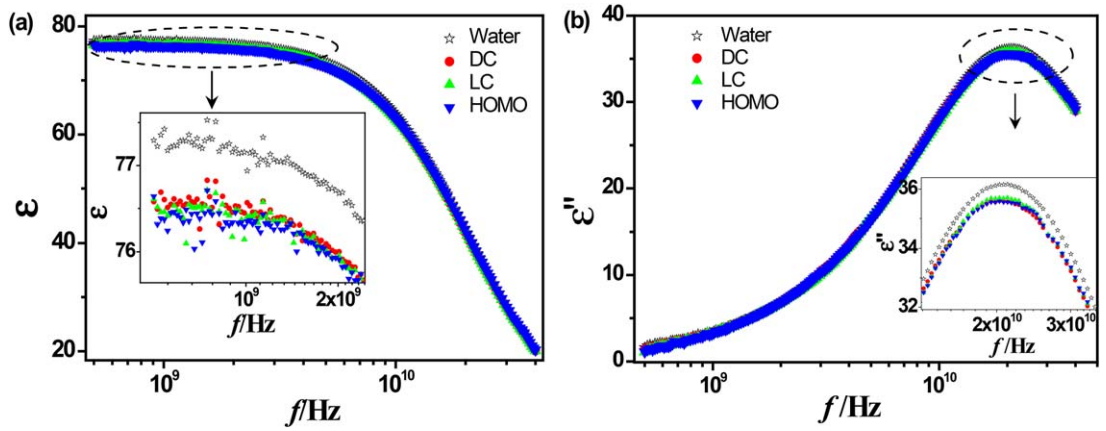

FIGURE 2 Dielectric spectroscopy of PNIPAM microgel solution and water (a) dielectric constant and (b) loss at room temperature. [Color figure can be viewed at wileyonlinelibrary.com]

$$\varepsilon^* = \varepsilon_h + \frac{\Delta\varepsilon_{\text{free}}}{\left[1+(j\omega\tau_{\text{free}})^{\alpha_{\text{free}}}\right]^{\beta_{\text{free}}}} + \frac{\Delta\varepsilon_{\text{bound}}}{\left[1+(j\omega\tau_{\text{bound}})^{\alpha_{\text{bound}}}\right]^{\beta_{\text{bound}}}} \quad (1)$$

where ε_h is high frequency limit of permittivity, ω is the angular frequency, $j=(-1)^{1/2}$, $\Delta\varepsilon$ is dielectric strength, τ is relaxation time, α and β are the parameters indicating the distribution of relaxation time.[30] The subscripts *free* and *bound* represent the free and bound water, respectively. Usually, in studies of aqueous systems models with fewer number of fitting parameters are used, therefore, during the fitting process, we fixed some shape parameters ($\alpha_{\text{free}}=\beta_{\text{free}}=1$, $\alpha_{\text{bound}}=1$), that is, essentially, the Debye + Cole–Cole model (2) was used in the fitting process

$$\varepsilon^* = \varepsilon_h + \frac{\Delta\varepsilon_{\text{free}}}{1+(j\omega\tau_{\text{free}})} + \frac{\Delta\varepsilon_{\text{bound}}}{\left[1+(j\omega\tau_{\text{bound}})\right]^{\beta_{\text{bound}}}}. \quad (2)$$

Because Ohmic conduction is pronounced at low frequencies and in the system with high conductivity, the correction for Ohmic conductance is no longer considered here. All the dielectric spectra are well fitted by this equation. As a representative case, the frequency dependence of the dielectric loss ε'' for HOMO microgel system was shown in Figure 3. The hollow circles represent raw data, and the dotted line represents the contribution of free or bound water. The inset is the enlargement of the dielectric loss of bound water. As can be seen from the inset, the characteristic frequency and strength of the dielectric loss of bound water change with the temperature. That is to say, with the collapse of microgel, the interaction between bound water and PNIPAM changed obviously, proving that the bound water can reflect the volume phase transition of microgel. This speculation is also confirmed by the temperature dependences of the dielectric parameters in the following Figure 4.

Hydration Dynamic and the Distinction of Different Microgels

Figure 4 shows the temperature dependences of dielectric strength and relaxation time for free and bound water. It is known to all that below the VPTT, the PNIPAM microgel is in highly swollen state due to the hydrogen bonding between amide groups and bound water; when the temperature rises to VPTT, the microgel collapses, expelling most of its water to the bulk due to the hydrophobic behavior of the pendent isopropyl groups as well as that of the backbone.[15] In Figure 4(a), the temperature dependences of $\Delta\varepsilon_{\text{free}}$ for the three microgels are similar, but they are obviously different from that of pure water. Besides, dielectric strength of free water $\Delta\varepsilon_{\text{free}}$ is much larger than that of bound water $\Delta\varepsilon_{\text{bound}}$, this is because most of the water in microgel system is free water, whose amount is far more than that of bound water. The difference in the dielectric strength between the pure water and the free water (i.e., $\Delta\varepsilon_{\text{water}}$-$\Delta\varepsilon_{\text{free}}$) for all the three microgels turns at 32 °C (VPTT, dotted line), revealing that the crosslink density distribution does not affect the VPTT of microgel. When the temperature rises above VPTT, $\Delta\varepsilon_{\text{free}}$ gradually approaches to that of pure water (triangular gray shadow). This indicates that bound water is expelled to the

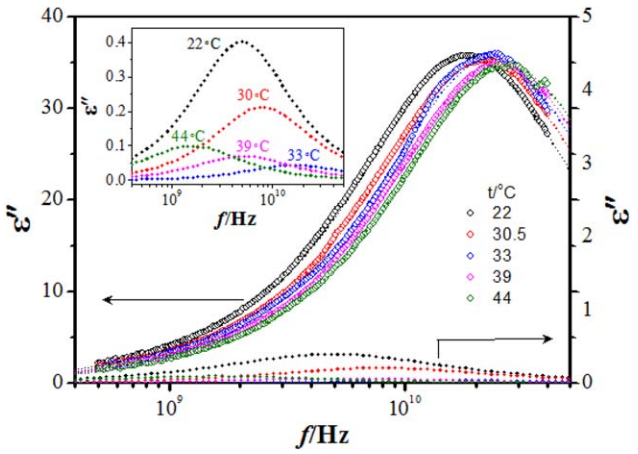

FIGURE 3 Frequency dependence of the derivative dielectric loss of HOMO PNIPAM microgel at different temperatures. The hollow circles are the raw data. The dashed lines are the contribution of bound and free water. The inset shows the enlarged view of the contribution of bound water. [Color figure can be viewed at wileyonlinelibrary.com]

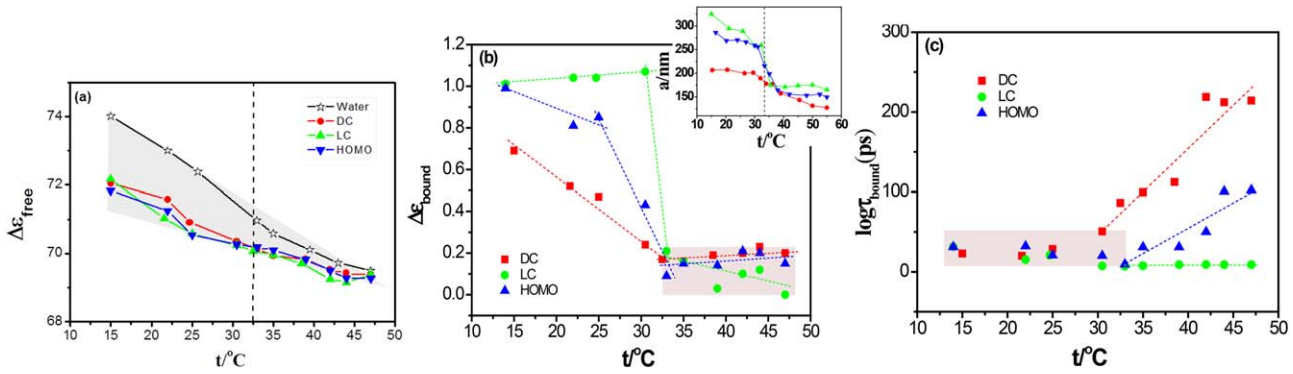

FIGURE 4 Temperature dependence of dielectric parameters for (a) free and (b,c) bound water. The triangular gray shadow in (a) shows that the dielectric strength of free water $\Delta\varepsilon_{free}$ gradually approaches to that of pure water. The inset of (b) is the temperature dependence of the size for microgel, whose data are from our previous study.[25] [Color figure can be viewed at wileyonlinelibrary.com]

bulk and the amount of free water is gradually close to that of pure water, proving the collapse process of microgel from the view of solvent. Note that the dielectric strength of the free water is nearly the same, indicating that the three kinds of microgel cannot be distinguished from the view of free water.

However, the three kinds of microgels can be distinguished by the dielectric increment and relaxation time of bound water, $\Delta\varepsilon_{bound}$ and τ_{bound}. Figure 4(b,c) show that the temperature dependences of $\Delta\varepsilon_{bound}$ and τ_{bound} for all the three microgels change at 32 °C, which further confirmed that the crosslinking density distribution does not affect the VPTT. In addition, at $t <$ VPTT, the $\Delta\varepsilon_{bound}$ for the three microgels follows the relation LC > HOMO > DC, which means that the numbers of bound water in HOMO and LC microgels are greater than that in DC microgel. Because the amount of bound water actually reflects the water content inside the microgel, the above relation indicates that the LC and HOMO microgels are more swollen than DC microgel. This is because that the microgel core dominates the swelling capability of microgel, and the microgel with lightly crosslinked core is more swollen.[26] This result is consistent with the relation of the size of the three microgels [inset in Fig. 4(b)] which was obtained from our previous study.[25] Besides, another interesting result is that the temperature dependence of $\Delta\varepsilon_{bound}$ for these three microgels is obviously different from each other, and the sharpness of their transition follows: LC > HOMO > DC, indicating that the cross-linking density distribution plays an important role in the volume phase transition of microgels. Tanaka[31] et al. thought that the swelling of gel is essentially achieved by swelling of loosely crosslinked domains alone; thus, the volume phase transition of gel with heterogeneous structure should be more discontinuous (i.e., the volume phase transition becomes more obvious if the inhomogeneity of microgel network is pronounced). This is partly confirmed by Figure 4(b). In short, the spatial distribution of cross-linking density does not influence the VPTT, but influence the continuity of volume phase transition.[32,33]

Figure 4(c) shows that τ_{bound} of the three microgels remains a constant at lower temperatures (shadow), and exhibits different trends at higher temperatures: τ_{bound} of DC and HOMO microgels increases with temperature, while that of LC microgel remains unchanged, which suggests that the rotational dynamics of bound water is closely related to the structure of microgel. In general, as temperature increases, the dynamics of bound water is affected by two factors: on the one hand, the enhanced thermal movement will hinder the orientation of water, and on the other hand, the increasing temperature will weaken the strength of hydrogen bonding between water and the solute PNIPAM, promoting the orientation of water. Therefore, the τ_{bound} curve should be a balanced result of the above two aspects. It is preliminarily concluded that the differences between the three microgels are related to the location of water molecules in the microgel (the water inside the microgel tends to distribute on the space with smaller crosslink density, which is beneficial to interact with PNIPAM because of less steric hindrance). Although we are unable to give further understanding about the different orientation dynamics of the three microgels at present, these above interesting results proves that the three kinds of microgels can be distinguished from the view of bound water.

Quantification of Solvent Water in Microgel

To quantitatively describe the hydration dynamic of microgel, one can calculate the concentration of water at each temperature by Cavell equation,[34] which describes the relation between dielectric strength and concentration of the dipoles in the system,

$$\frac{2\varepsilon_l+1}{\varepsilon_l}\Delta\varepsilon_i = \frac{N_A c_i}{k_B T \varepsilon_0}\mu_i^2 \quad (3)$$

where ε_l is the permittivity at low-frequency limit; ε_0 is the permittivity of vacuum; N_A, k_B, and T are the Avogadro constant, Boltzmann constant, and absolute temperature, respectively; c_i and μ_i is the molar concentration and dipole moment of the species i in mixtures, respectively. Thus, the relationship between the dielectric strength and concentration of free water

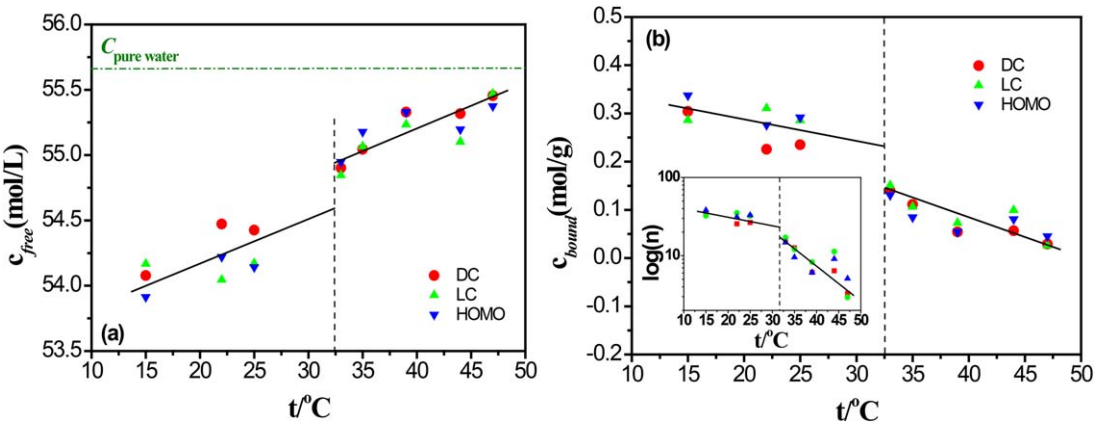

FIGURE 5 Temperature dependence of concentration for (a) free water and (b) bound water. The green dot–dash line in (a) represents the molar concentration of pure water. The inset is the number of bound water *n* on each monomer. [Color figure can be viewed at wileyonlinelibrary.com]

in the microgel solution ($\Delta\varepsilon_{free}$, c_{free}) and that of pure water ($\Delta\varepsilon_w^0$, $c_w^0 = \rho_w^0/M_w$) is derived as

$$c_{free} = \frac{\Delta\varepsilon_{free}\rho_w^0}{\Delta\varepsilon_w^0 M_w} \quad (4)$$

where ρ_w^0 and M_w are the density and the molar mass of pure water, respectively. In theory, if the concentration of PNIPAM microgel solution c_{PNIPAM} is known, the number of bound water in per microgel Z can be described as follows:

$$Z = \frac{c_{bound}}{c_{PNIPAM}} = \frac{c_w - c_{free}}{c_{PNIPAM}} = \left(\frac{w}{M_w} - c_{free}\right)\frac{M_{PNIPAM}}{w_{PNIPAM}} \quad (5)$$

where c_{bound} and c_w are the molar concentration of bound water and the water in the microgel solution; w is the mass concentration of water in microgel solution; M_{PNIPAM} and w_{PNIPAM} are the molecular weight and mass concentration of PNIPAM microgel. Unfortunately, because M_{PNIPAM} is unknown, we cannot calculate the number of bound water molecules in each PNIPAM microgel. Despite this, since w_{PNIPAM} is known, the molar concentration of bound water in per unit mass microgel (mol/g) can be obtained.

Figure 5 shows the concentration of free and bound water (c_{free} and c_{bound}) obtained from eq. (4–5). Similar to the temperature dependence of $\Delta\varepsilon_{free}$, c_{free} [Fig. 5(a)] increases with temperature and gradually closes to the concentration of pure water ($C_{pure\ water} = 55.6$ mol/L, green dotted line). This suggests that water molecules continuously release from the PNIPAM microgel network, leading to a decrease in the concentration of bound water [Fig. 5(b)]. In addition, both the concentration of free and bound water in Figure 5(a,b) shows a significant change at about 32 °C, suggesting the volume phase transition. Now let us focus on the concentration of bound water c_{bound}. c_{bound} reduces from 0.3 mol/g (15 °C) to about 0.03 mol/g (47 °C). Considering the molecular weight of monomer NIPAM (113.18), the number of bound water on each monomer *n* is obtained as shown in the inset, reducing from 34 to 3 with the increasing of temperature. This value is greater than the number of hydrated number in previous studies of PNIPAM chain (11-0 of Shikata and coworkers[15–17] and 8-2 of Philipp et al.[21]), suggesting that for microgel networks the bound water not only includes the water molecules that bond to the monomer, but also includes the water molecules that are bound in the network. This difference reveals that the dynamics of the water molecules which do not interact with PNIPAM but are limited in the network is also different from that of the bulk water.

CONCLUSIONS

We developed an approach to quantitatively calculate the hydration number of microgel and studied the hydration dynamic of thermosensitive microgel from the view of solvent by dielectric spectroscopy. We found that hydration number on each monomer unit reduced from 34 at low temperatures to 3 at high temperatures, proving the volume phase transition from the view of solvent. In addition, it was found that the crosslink density distribution does not affect the VPTT of microgel, but can significantly affect the orientation dynamics of the solvent water, especially the bound water. Therefore, the three kinds of microgels can be distinguished by the dielectric parameters of bound water.

This study provides possibility for the quantification of water molecules in complex process, which will undoubtedly help us to understand the structure and dynamics of natural or synthetic macromolecules, as well as some complex biological mechanisms.

ACKNOWLEDGMENTS

The authors thank Dr. Shaojie Zhao of Beijing Normal University for providing the facilities for the dielectric measurements. This work was supported by the National Natural Science Foundation of China (grant nos. 21173025, 21473012, and 21673002) and the Major Research Plan of NSFC (grant no. 21233003).

REFERENCES AND NOTES

1 M. Chaplin, *Nat. Rev. Mol. Cell Biol.* **2006**, *7*, 861.

2 K. Oda, R. Kodama, T. Yoshidome, M. Yamanaka, Y. Sambongi, M. Kinoshita, *J. Chem. Phys.* **2011**, *134*, 025101.

3 Y. Miyashita, T. Wazawa, G. Mogami, S. Takahashi, Y. Sambongi, M. Suzuki, *Biophys. J.* **2013**, *104*, 163.

4 K. A. Dill, J. L. Maccallum, *Science* **2012**, *338*, 1042.

5 L. B. Sagle, Y. Zhang, V. A. Litosh, X. Chen, Y. Cho, P. S. Cremer, *J. Am. Chem. Soc.* **2009**, *131*, 9304.

6 J. Wang, B. Liu, G. Ru, J. Bai, J. Feng, *Macromolecules* **2016**, *49*, 234.

7 A. Płaczek, G. Hefter, H. M. Rahman, R. Buchner, *J. Phys. Chem. B* **2011**, *115*, 2234.

8 M. Bešter-Rogač, A. Stoppa, J. Hunger, G. Hefter, R. Buchner, *Phys. Chem. Chem. Phys.* **2011**, *13*, 17588.

9 W. Wachter, G. Trimmel, R. Buchner, O. Glatter, *Soft Matter.* **2011**, *7*, 1409.

10 J. Hunger, S. Niedermayer, R. Buchner, G. Hefter, *J. Phys. Chem. B* **2010**, *114*, 13617.

11 R. Buchner, G. Hefter, *Phys. Chem. Chem. Phys.* **2009**, *11*, 8984.

12 M. Lukšič, R. Buchner, B. Hribarlee, V. Vlachy, *Macromolecules* **2009**, *42*, 4337.

13 R. Buchner, *Pure Appl. Chem.* **2008**, *80*, 1239.

14 J. Barthel, R. Buchner, P. N. Eberspächer, M. Münsterer, J. Stauber, B. Wurm, *J. Mol. Liquids* **1998**, *78*, 83.

15 Y. Ono, T. Shikata, *J. Am. Chem. Soc.* **2006**, *128*, 10030.

16 Y. Ono, T. Shikata, *J. Phys. Chem. B.* **2007**, *111*, 1511.

17 Y. Satokawa, T. Shikata, F. Tanaka, X-p. Qiu, F. M. Winnik, *Macromolecules* **2009**, *42*, 1400.

18 M. Shibayama, M. Morimoto, S. Nomura, *Macromolecules* **1994**, *27*, 5060.

19 M. Shibayama, S-y. Mizutani, S. Nomura, *Macromolecules* **1996**, *29*, 2019.

20 H. Kogure, S. Nanami, Y. Masuda, Y. Toyama, K. Kubota, *Colloid Polym. Sci.* **2005**, *283*, 1163.

21 M. Philipp, K. Kyriakos, L. Silvi, W. Lohstroh, W. Petry, J. K. Krüger, C. M. Papadakis, P. Müller-Buschbaum, *J. Phys. Chem. B.* **2014**, *118*, 4253.

22 M. Yang, C. Liu, Y. Lian, K. Zhao, D. Zhu, J. Zhou, *Soft Matter.* **2017**, *13*, 2663.

23 M. Yang, K. Zhao, *Soft Matter.* **2016**, *12*, 4093.

24 C. Wu, S. Zhou, S. C. Au-yeung, S. Jiang, *Angew. Makromol. Chem.* **1996**, *240*, 123.

25 W. Su, K. Zhao, J. Wei, T. Ngai, *Soft Matter.* **2014**, *10*, 8711.

26 J. Wei, Y. Li, T. Ngai, *Colloids Surf. A Physicochem. Eng. Aspect* **2015**, *489*, 122.

27 U. Kaatze, *J. Chem. Eng. Data.* **1989**, *34*, 371.

28 S. Nakano, Y. Sato, R. Kita, N. Shinyashiki, S. Yagihara, S. Sudo, M. Yoneyama, *J. Phys. Chem. B* **2012**, *116*, 775.

29 M. Fullbrandt, E. Ermilova, A. Asadujjaman, R. Hölzel, F. F. Bier, R. von Klitzing, A. Schönhals, *J. Phys. Chem. B* **2014**, *118*, 3750.

30 M. Fang, J. Gao, S. Wang, Y. Lian, K. Zhao, *Chin. Sci. Bull.* **2010**, *55*, 1246.

31 T. Tanaka, M. Annaka, *Ann. Rev. Mater. Res.* **1992**, *64*, 243.

32 R. Acciaro, T. Gilányi, I. Varga, *Langmuir* **2011**, *27*, 7917.

33 S. Seiffert, *Macromol. Rapid Commun.* **2012**, *33*, 1135.

34 E. Cavell, P. Knight, M. Sheikh, *Faraday Soc.* **1971**, *67*, 2225